

## TWO-DIMENSIONAL HYPERCHAOTIC MAP FOR CHAOTIC OSCILLATIONS

Oleh Krulikovskyi<sup>1,2</sup>, Serhii Haliuk<sup>1</sup>, Ihor Safronov<sup>1</sup>, Valentyn Lesynskyi<sup>1</sup>

<sup>1</sup>Yuriy Fedkovych Chernivtsi National University, Department of Radioengineering and Information Security, Chernivtsi, Ukraine, <sup>2</sup>Ștefan cel Mare University of Suceava, Suceava, Romania

**Abstract.** This manuscript explores a two-dimensional hyperchaotic map for generating chaotic oscillations. Hyperchaotic maps are finding increasing applications in various scientific and technological fields due to the unique properties of their generated oscillations. The studied map, based on two interconnected piecewise-linear functions, is one of the simplest for generating oscillations with a predetermined distribution of values across a continuous parameter space. This simplicity allows for wide applicability in various contexts. The paper presents simulation results demonstrating control over the parameters of the dynamic modes. Building upon these modeling results, a two-dimensional hyperchaotic system is implemented using an electric circuit. The chosen map is attractive due to its inherent simplicity and ease of parameter control. By adjusting these parameters, the distribution of the generated signal's values can be manipulated. The circuit consists of two symmetrical sections connected via feedback loops, employing four amplifiers with variable gain. The gain values act as the circuit's implementation of the control parameters. Chaotic oscillations are generated by applying a delayed clock signal from an external square wave generator to circuit elements. The obtained experimental results exhibit excellent agreement with the simulation data.

**Keywords:** hyperchaotic map, chaotic oscillations, variable distribution, circuit implementation

### DWUWYMIAROWA MAPA HIPERCHAOTYCZNA DLA CHAOTYCZNYCH OSCYLACJI

**Streszczenie.** W artykule przedstawiono badania dwuwymiarowej mapy hiperchaotycznej pod kątem oscylacji chaotycznych. Mapy hiperchaotyczne są coraz częściej wykorzystywane w różnych dziedzinach nauki i techniki ze względu na właściwości generowanych przez nie oscylacji. Mapa oparta na dwóch wzajemnie powiązanych, fragmentarycznie skorelowanych funkcjach jest jedną z najprostszych, które mogą generować oscylacje o zadanym rozkładzie wartości dla ciągłej przestrzeni parametrów sterujących. Umożliwia to szerokie zastosowanie takiego systemu w wielu zastosowaniach. Pokazano wyniki symulacyjnego sterowania parametrami modów dynamicznych. Na podstawie wyników modelowania zaprojektowano implementację obwodu elektrycznego dwuwymiarowego układu hiperchaotycznego. Wybór systemu wynika z jego prostoty i łatwości sterowania parametrami. Sterowanie parametrami systemu pozwala na zmianę rozkładu wartości generowanych sygnałów. Układ składa się z dwóch symetrycznych części połączonych ze sobą sprzężeniami zwrotnymi, opartych na 4 wzmacniaczach o zmiennym wzmacnieniu. Wartość wzmacnienia jest realizacją obwodu parametrów sterujących. Generowanie chaotycznych oscylacji następuje po postarzeniu do elementów opóźniających sygnału zegarowego z zewnętrznego generatora fali prostokątnej. Uzyskane wyniki eksperymentalne wykazują pełną zgodność z wynikami symulacji.

**Słowa kluczowe:** mapa hiperchaotyczna, oscylacje chaotyczne, rozkład zmiennych, implementacja obwodu

### Introduction

During the active development of information technology diversity and complexity of information security problems are continuously growing [2]. Data volume is continuously increasing, which causes an urgent necessity for high-quality generators of special signals to process and protect them. Therefore, a major focus of research in cryptography and telecommunications is the improvement and development of new approaches based on truly random and pseudorandom numbers [22]. A significant part of information processing issues can be solved through chaotic signals generated by nonlinear systems. Despite being deterministic, chaotic systems have unpredictable long-term behavior induced by instability which causes high sensitivity to initial conditions and parameters. This unique property spurred scientists to leverage chaos for various applications, including cryptographic algorithms, secure and covert communication [3, 9].

There are a large number of chaotic systems possessing different qualities which makes them not equally applicable to protect data. To be suitable for cryptography a chaotic system must correspond to strict criteria which the simplest systems are not able to meet [1]. In cryptographic applications, preference should be given to systems that produce time series whose values have a dense and uniform distribution across the continuous range of control parameters [7].

Ring-coupled discrete multidimensional maps are improved versions of one-dimensional linear piecewise functions [6, 13]. Implementation of such systems based on a CPU or FPGA demonstrates they possess excellent characteristics [5, 11].

Schematic implementation of ring-coupled maps presents a challenge due to the branching operators used in their defining mathematical models [8]. The general method for constructing discrete chaotic systems is described in [16]. The basis of the circuits is capacitors or sample-and-hold branches as memory elements, operational amplifiers for analog realization

of mathematical operations, and switches for controlling the circuit's operation. The state of circuits of discrete generators is changing under the influence of a clock signal. Any real circuit, including a generator of chaotic oscillations, is continuously influenced by thermal noise. This means that the chaotic dynamics will take place only in scale compared with the size of the attractor [20, 21]. Due to the inherent sensitivity of chaos, these noise disturbances will randomly alter the oscillation trajectory. Consequently, a physical oscillator exhibits chaotic behavior with additional random and continuous stochastic effects [4, 19].

To achieve a simpler schematic implementation for the random number generator based on ring-coupled maps, we propose utilizing a two-dimensional hyperchaotic map [10]. Simplification is achieved due to the absence of branching operators in the mathematical model. At the same time, the possibility of obtaining chaotic oscillations with a predetermined distribution of values for a continuous range of control parameters remains.

The article is organized as follows. Section 1 covers the mathematical model, bifurcation diagrams, and Lyapunov exponents of a two-dimensional hyperchaotic system. Section 2 details the design, components, operation, and experimental results of a developed generator circuit. The conclusions are presented in Section 3.

### 1. Description of the hyperchaotic system

Hyperchaotic system under study is a two-dimensional discrete chaotic map, described by the following equations [10]:

$$\begin{cases} x(n+1) = a_1x(n) - b_1|y(n)| + 1 \\ y(n+1) = a_2y(n) - b_2|x(n)| + 1 \end{cases} \quad (1)$$

where  $a_1$ ,  $a_2$ ,  $b_1$  and  $b_2$  is system control parameters. To simplify the demonstration of chaotic modes in this paper, we assume that the control parameters are determined by the following rule:

$$\begin{cases} a_1 = a_2 = a \\ b_1 = b_2 = b \end{cases} \quad (2)$$



Dimension of the system (1) can be increased using a ring or mixed connections. In the case of a ring connection, system (1) will take the form:

$$\begin{cases} x_1(n+1) = ax_1(n) - b|x_2(n)| + 1 \\ x_2(n+1) = ax_2(n) - b|x_3(n)| + 1 \\ x_3(n+1) = ax_3(n) - b|x_4(n)| + 1 \\ \vdots \\ x_i(n+1) = ax_i(n) - b|x_1(n)| + 1 \end{cases} \quad (3)$$

where  $i$  – dimension of the system.

## 2. Analysis of the hyperchaotic system

System (1) can be chaotic or hyperchaotic depending on the value of parameters  $a$  and  $b$ . Bifurcation diagram and Lyapunov exponents analysis are conventionally used to determine modes of oscillations. These methods also allow us to determine the range of control parameters and oscillation values for different modes. Knowing the ranges of parameters within which chaotic or hyperchaotic oscillations are possible has significant applied value. When the largest Lyapunov exponents is positive, chaotic oscillations occur in the system.

Hyperchaos occurs when there are two Lyapunov exponents greater than zero. In other cases, the oscillations will have a periodic structure or the system will converge to a fixed point [23].

The bifurcation and Lyapunov exponents diagrams of system (1) are shown in Fig. 1. Fig. 1b and 1d reveal a wide range of control parameters that can induce chaos and hyperchaos in the system. Within the parameters ranges  $a = [-1; 0.48]$ ,  $b = 1.493$  and  $a = [0.01]$ ,  $b = [1.42; 1.989]$ , no periodic windows are detected. The distribution of the time series is continuous between the minimum and maximum values (see Fig. 1a, c). This continuous range of control parameters for generating non-periodic oscillations allows for the development of a random number generator based on a discrete hyperchaotic system implementation. As shown in Fig. 1b, when  $a = -0.95$ ,  $b = 1.493$ , one Lyapunov exponent is positive  $\lambda_1 = 0.33$ , while the second is negative  $\lambda_2 = -0.048$ , which indicates the presence of chaotic oscillations in the system.

To analyze the behavior and interdependence between output variables  $x(n)$  and  $y(n)$ , chaotic system phase portraits are studied as shown in Fig. 2.

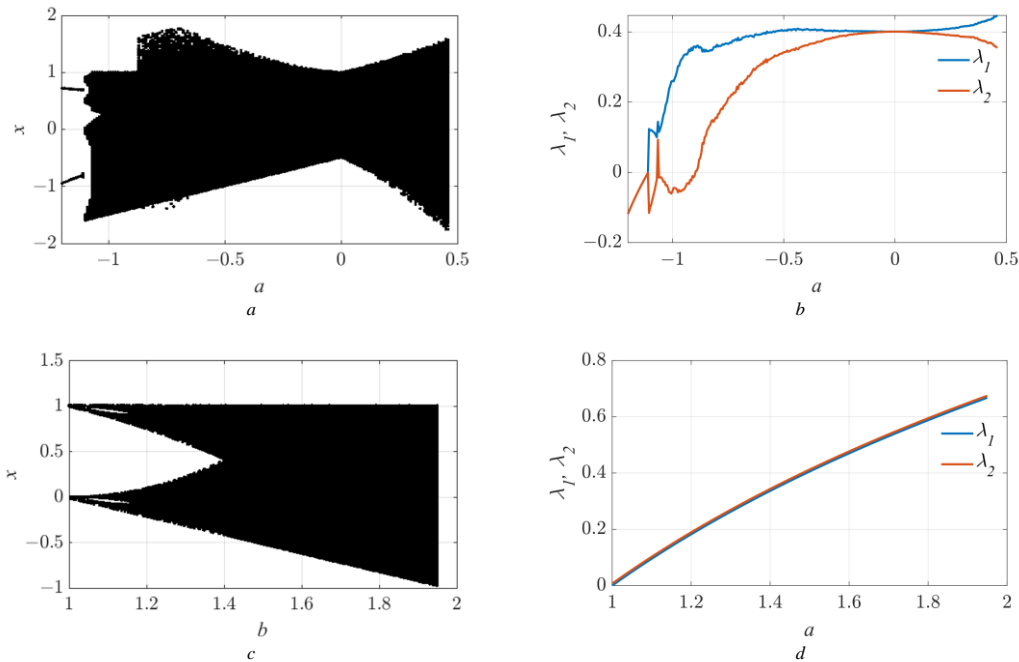


Fig. 1. Two-dimensional map: bifurcation diagram – (a), Lyapunov exponent diagram as function of parameter  $a$  at  $b = 1.493$  – (b); bifurcation diagram – (c), Lyapunov exponent diagram as function of parameter  $b$  at  $a = 0.01$  – (d)

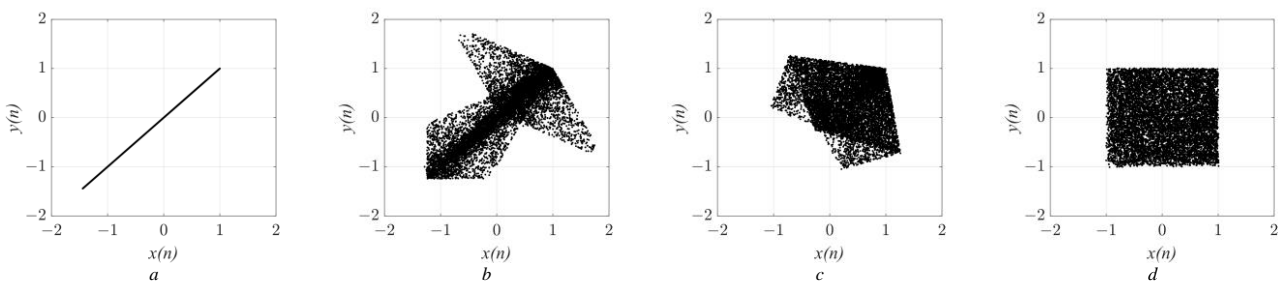


Fig. 2. The phase portraits of map (1) in chaotic regime at  $a = -0.95$ ,  $b = 1.493$  – (a); in hyperchaotic regimes at:  $a = -0.75$ ,  $b = 1.493$  – (b);  $a = 0.23$ ,  $b = 1.493$  – (c);  $a = 0.01$ ,  $b = 1.98$  – (d)

When  $a = -0.95$ ,  $b = 1.493$ , the chaotic system (1) has one positive Lyapunov exponent. In this mode system produces identical oscillations and can be considered as two connected, identical subsystems that are in complete synchronization (Fig. 2a). Non-linear conversion function  $x(n+1) = f(x(n))$  is piecewise linear map which consists of two two piecewise function (Fig. 3a).

When parameter  $a$  increases to  $a = -0.75$ ,  $b = 1.493$  two Lyapunov exponents are greater than zero ( $\lambda_1 = 0.369$ ,  $\lambda_2 = 0.21$ ), which means that hyperchaos appears with phase portrait as shown in Fig. 2b. With a further increase in  $a$ , the system (1) remains hyperchaotic (see Fig. 2c).

An interesting case is the hyperchaotic regime at  $a \rightarrow 0$ ,  $b = 1.493$  in which both Lyapunov exponents are almost equal. The phase portrait exhibits a square-like region densely populated with dots (Fig. 2d). This indicates statistical independence of two variables  $x(n)$  and  $y(n)$ . Detailed analysis of iterative diagrams (Fig. 3b and c) suggests that the system (1) is cross-connected two tent maps with weak feedback in the form of addends  $ax(n)$  and  $ay(n)$ .

Analysis of test suites for pseudorandomness (eg, NIST or Diehard tests [15, 18]) reveals that the key requirement to sources of randomness in cryptography is uniform distribution of generated numbers. Histograms of the chaotic timeseries

of system (1) are shown in Fig. 4. A uniform distribution is only observed for the case with  $a = -0.0001$ ,  $b = 1.998$  (Fig. 4c).

A common method for randomizing chaotic time series involves rejecting several high-order bits in their binary representation [3]. This is because the higher-order bits significantly influence the formation of the phase portrait and the distribution of time series values. At the same time, the least significant bits ideally exhibit an unbiased balance between “0” and “1”, improving the randomness of the generated sequence. An alternative approach to improve the value distribution involves increasing the dimensionality according to equation (3) using cross-connections [5].

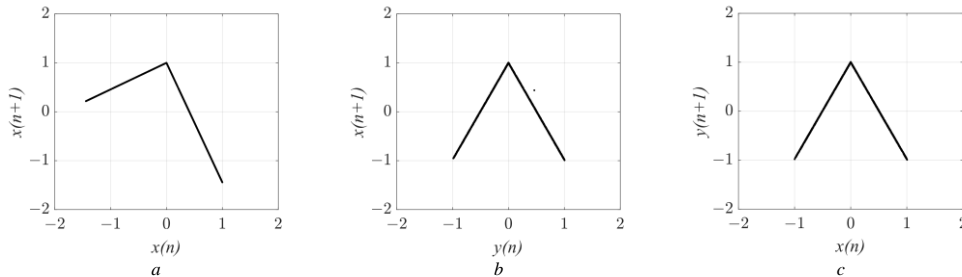


Fig. 3. Graphical representation of nonlinear transformation functions at  $a = -0.95$ ,  $b = 1.493$  - (a);  $a = 0.01$ ,  $b = 1.98$  - (b) and (c)

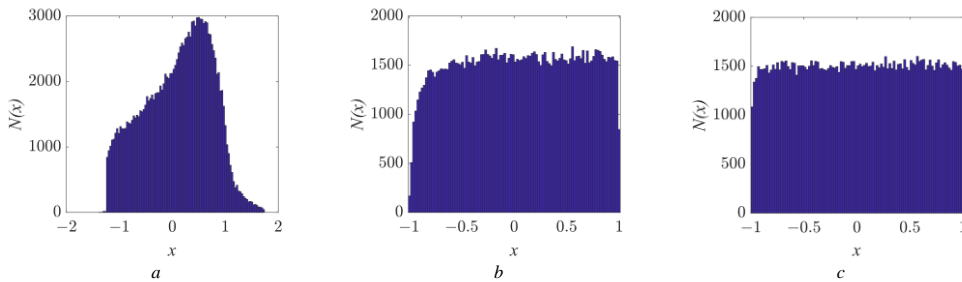


Fig. 4. Phase portrait and histogram distribution system (1): at  $a = -0.75$ ,  $b = 1.493$  - (a);  $a = 0.01$ ,  $b = 1.98$  - (b);  $a = 0.0001$ ,  $b = 1.998$  - (c)

### 3. Electrical circuit and experiment

Only analog dynamical system can generate truly chaotic signals [23]. In case of computer-based realization, regardless of the calculation format, chaotic signals will be distorted by rounding and timeseries become cyclic, due to operating in the finite field [12]. When implementing chaotic systems as electronic circuits, the precision of manufactured elements and disturbances caused by temperature fluctuations and other physical factors can impact their behavior. This can lead to discrepancies between real-world circuit behaviour and simulation results. While integral designs offer the most stable and accurate results, they come at a higher initial cost. Therefore, to study the basic modes of operation of the nonlinear system (1), this work utilized discrete elements (e.g., resistors, capacitors) in the circuit design.

#### 3.1. Electrical circuit

To implement (1) as an electronic circuit, it requires rescaling the system into a form suitable for hardware tools. We achieve this by performing the following substitution:

$$\begin{aligned} u(n) &= E_u x(n) \\ v(n) &= E_v y(n) \end{aligned} \quad (4)$$

where  $E_u, E_v$  is the regulation voltage that is set for  $u(n)$  and  $v(n)$  using two separate power supplies.

By tuning  $E_u, E_v$  it is possible to regulate the amplitudes of oscillation in circuit.

In order to shift the values of parameter  $a_1$  and  $a_2$  to positive ranges, we introduce new parameters  $A_1$  and  $A_2$  such that:

$$\begin{aligned} a_1 &= A_1 - 1 \\ a_2 &= A_2 - 1 \end{aligned} \quad (5)$$

where  $A_1$  and  $A_2 > 0$ .

Considering (4) and (5), system (1) takes the following form:

$$\begin{cases} u(n+1) = (A_1 - 1)u(n) - B_1|v(n)| + E_u \\ v(n+1) = (A_2 - 1)v(n) - B_2|u(n)| + E_v \end{cases} \quad (6)$$

where  $A_1, A_2, B_1$  and  $B_2$  - are new parameters of the system. In this way, we obtained a system of equations that can be trivially implemented in the form of an electronic circuit.

For the experimental study of chaotic oscillations generated by a hyperchaotic system (6), an electrical circuit shown in Fig. 5 was developed. As well as the mathematical model (6), the scheme generally consists of two coupled parts. Separately, each of the parts consists of a block of sampling and holding devices, a block of setting  $E_u$  or  $E_v$ , a full-wave rectifier and a block of mathematical operations based on operational amplifiers.

Setting the regulation voltage for each part is performed by applying a voltage of  $\pm 12$  volts to the variable resistors: for  $E_u$  it is R17, for  $E_v$  it is R20. Setting the value of control parameters  $A_1, A_2, B_1, B_2$  also implemented on the basis of variable resistors. Specifically, resistors R33 and R6 are used to tune  $A_1$  and  $A_2$  respectively.

For absolute value operation  $|v(n)|$ , a full-wave rectifier is used, consisting of two operational amplifiers (left part of U1) and diodes D1 and D2 (Fig. 5). Similarly, for absolute value operation  $|u(n)|$ , another full-wave rectifier is implemented using U3 and diodes D3 and D4.

The sampling and holding function for both parts is implemented using two sample-and-hold chips LF398 and a logic inverter based on a 2N2222 transistor Q1. Blocks U4 and U5 are initialized with the values of  $u(n+1)$  and  $v(n+1)$ , respectively, on the rising edge of the clock signal (provided by the pulse generator). Conversely, blocks U6 and U7

are initialized with the values of  $u(n)$  and  $v(n)$ , respectively, on the rising edge of the inverted clock signal. This design ensures that during the first half period of the clock signal, capacitors C1 and C2 hold the values of  $u(n)$  and  $v(n)$  from the previous iteration. In the second half period, capacitors C3 and C4 capture the current values of  $u(n)$  and  $v(n)$ . Parameters  $B_1$  and  $B_2$  are set using variable resistors P31 and P32, respectively.

The specification and nominal values of all used components from Fig. 5 are given in table 1.

Table 1. Components and the nominal values of the circuit elements

Component	Specification
R1,R3,R5,R7,R8,R11-R16, R18, R19, R21-R30, R34-R36	10 kOm $\pm 5\%$
R6, R17, R20, R31, R32, R33	variable resistors, 20 kOm $\pm 5\%$
R2, R4, R9, R10	20 kOm $\pm 5\%$
D1-D4	1N4001
Q1	2N2222A
C1-C4	10 nF $\pm 5\%$
U1-U3	TL084
U4-U7	LF398

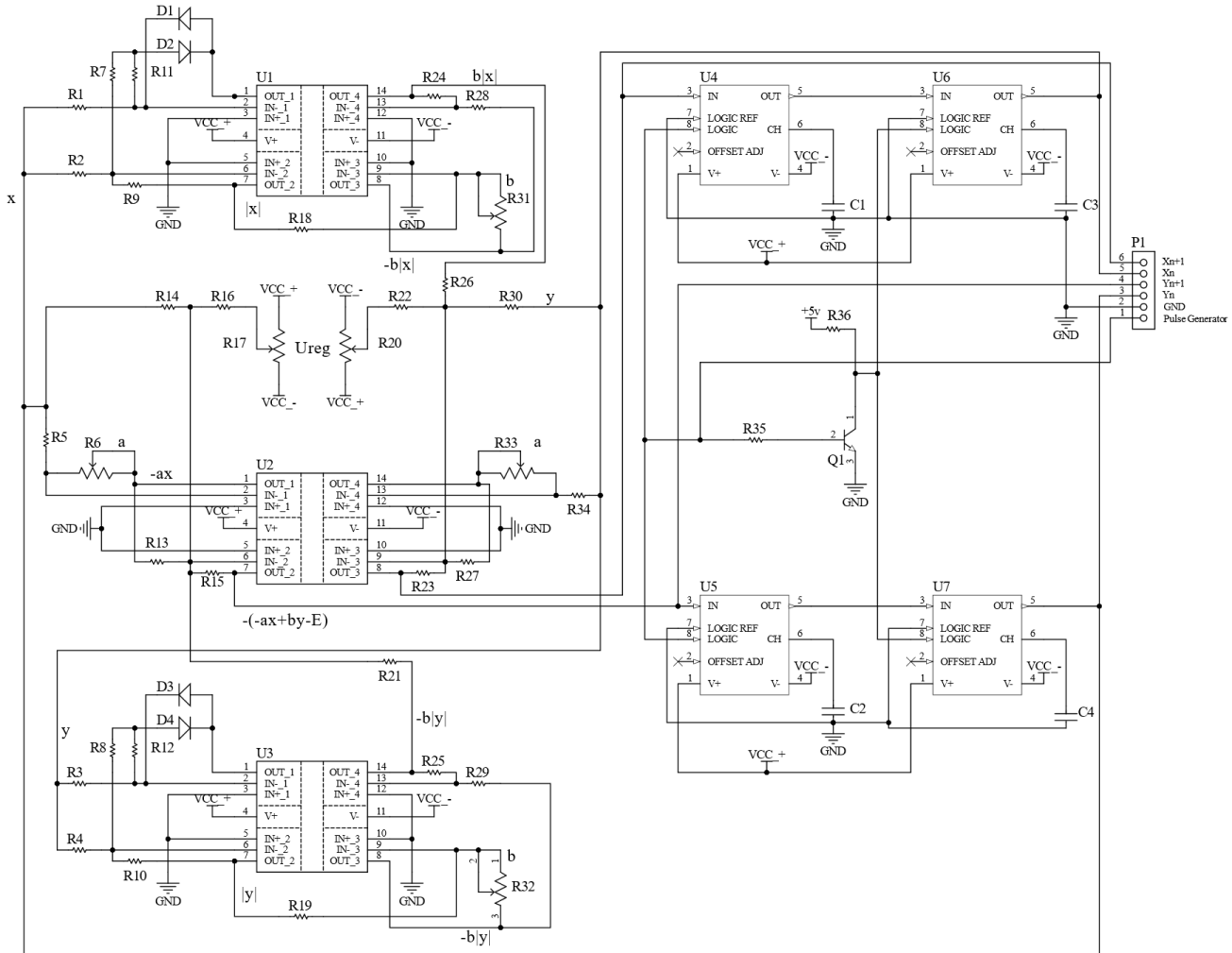


Fig. 5. Electrical circuit of chaotic generator (4)

The elements U1-U7 are powered by a bipolar 12-volt power supply. The inverter has a separate power supply that provides +5 volts to the base of the transistor through resistor R35. A clock signal is applied to switch between sample and hold states of chips U4-U7. The system will generate chaotic oscillations at the frequency of the clock signal. The frequency of the clock signal is less than 100 KHz because discrete general-purpose elements are used. At higher frequencies, the system will be unstable.

### 3.2. Experiment

To experimentally investigate the chaotic oscillator, we constructed a breadboard prototype using the components listed in table 1.

According to the specified requirements, we provide the corresponding power supply voltages. To demonstrate the generator's various chaotic operating modes, we set the clock signal frequency to 10 kHz. The experimental oscillograms of the generated signals are shown in Fig. 6.

While the experimental data for oscillations  $u(n)$  and  $v(n)$  appear random and unpredictable in Fig. 6a, b, c. The actual transformation function, as evidenced by the simulation results, is indeed piecewise linear as shown in Fig. 6d, e, f.

The phase portraits in Fig. 6g, h, i depict the hyperchaotic regimes of the oscillator, shown up to scaling factors  $E_u$  and  $E_v$  similar to Fig. 3.

To control the amplitude of the oscillations, parameters  $E_u$  and  $E_v$  were set as follows: Fig. 6a, d, g –  $E_u \approx E_v = -4$  V; Fig. 6b, e, h, c, f, i –  $E_u \approx E_v = -5.5$  V.

Analysis of numerical and experimental results shows that the schematic implementation of the hyperchaotic system preserves all its original properties, even when noise and other physical processes present.

The goal of further research is the development of a higher-speed circuit based on high-precision components and a comprehensive statistical study of the obtained chaotic oscillations and generator operating modes. This will ultimately lead to minimizing the influence of various physical processes on the generator's operation.

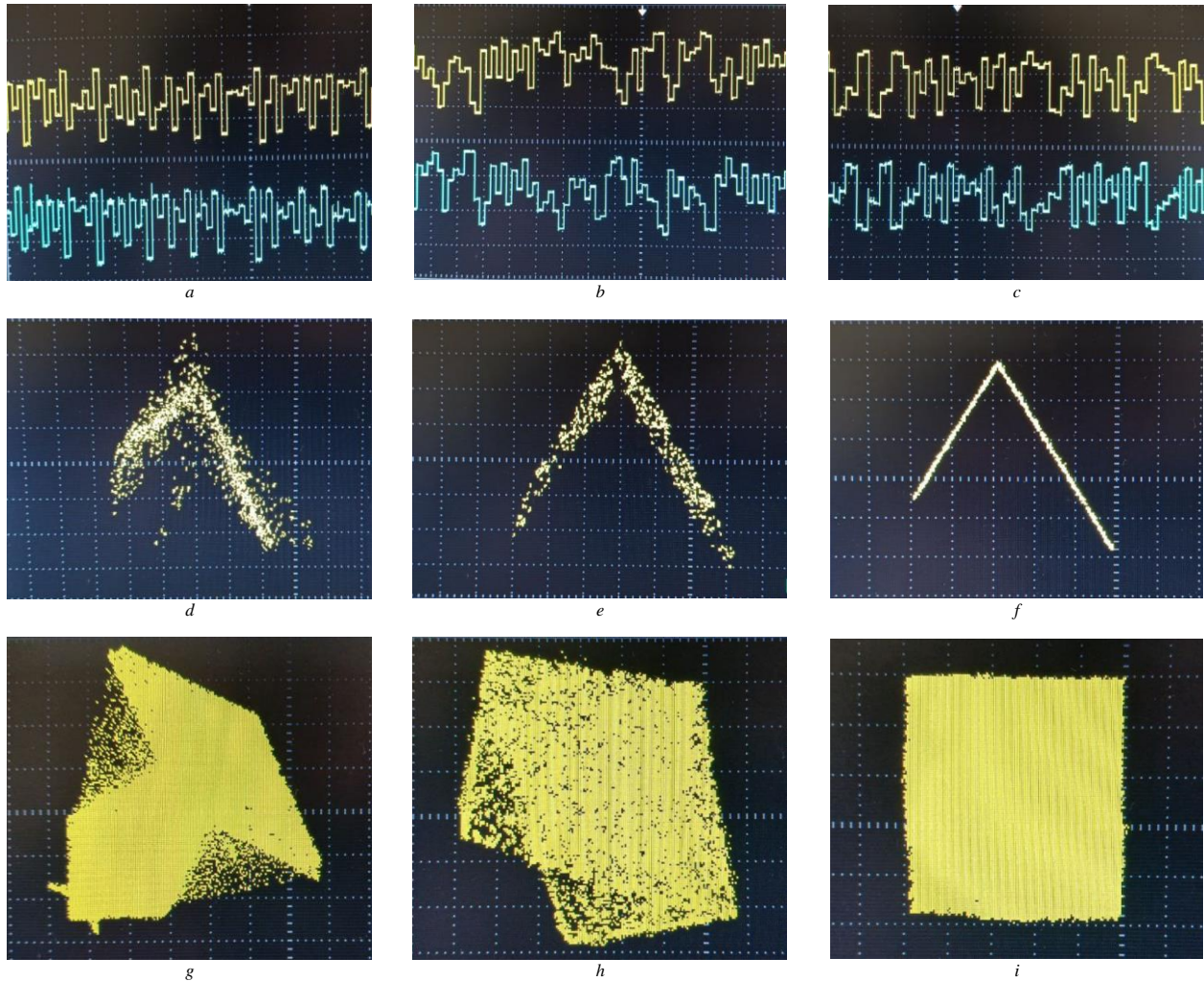


Fig. 6. Hyperchaotic oscillations:  $u(n)$  – upper signal,  $v(n)$  – lower signal – (a, b, c); nonlinear conversion function  $u(n) = f(v(n+1))$  – (d, e, f); phase portrait at:  $R31 \approx R32 \approx 14.93 \text{ kOm}$ ,  $R6 \approx R33 \approx 2.5 \text{ kOm}$  – (g);  $R31 \approx R32 \approx 12.3 \text{ kOm}$ ,  $R6 \approx R33 \approx 16.6 \text{ kOm}$  – (h);  $R31 \approx R32 \approx 12.3 \text{ kOm}$ ,  $R6 \approx R33 \approx 10.0 \text{ kOm}$  – (i)

#### 4. Conclusions

The study demonstrates that the system exhibits complex behavior across a wide range of control parameter values. Computer modeling revealed the system's ability to operate in both chaotic and hyperchaotic regimes. Adjusting parameters of system allows control over the distribution of generated timeseries, making it relevant for various applications.

Furthermore, a mathematical model suitable for circuit implementation was developed to explore the system's properties. This model was used to design an electronic circuit with discrete components. Experimental results of the resulting chaotic oscillator generator aligned well with the simulations. The influence of noise and parameters' mismatch was found to be minimal on the system's operation.

Future research will focus on improving the generator's performance by utilizing high-precision components.

#### References

- [1] Alvarez G., Shujun L.: Some basic cryptographic requirements for chaos-based cryptosystems. *International journal of bifurcation and chaos* 16(08), 2006, 2129–2151 [https://doi.org/10.1142/S0218127406015970].
- [2] Callegati F. et. al.: *Traffic Engineering: A Practical Approach*. Springer, 2022 [https://doi.org/10.1007/978-3-031-09589-4].
- [3] Corinto F. et. al.: Memristor-based chaotic circuit for pseudo-random sequence generators, *Proc. of 18th Mediterranean Electrotechnical Conference MELECON 2016*, Limassol, Cyprus, 2016 [https://doi.org/10.1109/MELCON.2016.7495319].
- [4] Endo T., Yokota J.: Generation of White Noise by Using Chaos in Practical Phase-Locked Loop Integrated Circuit Module. *IEEE International Symposium on Circuits and Systems ISCAS*, New Orleans, LA, USA 2007, 201–204 [https://doi.org/10.1109/ISCAS.2007.378311].
- [5] Garasym O. et. al.: How useful randomness for cryptography can emerge from multicore-implemented complex networks of chaotic maps. *Journal of Difference Equations and Applications* 23(5), 2017, 821–859 [https://doi.org/10.1080/10236198.2017.1287176].
- [6] Garasym O. et. al.: New Nonlinear CPRNG Based on Tent and Logistic Maps. *Complex Systems and Networks*. Lü J. et. al. (ed.): *Understanding Complex Systems*. Springer 2016 [https://doi.org/10.1007/978-3-662-47824-0\_6].
- [7] Garasym O. et. al.: Robust PRNG based on homogeneously distributed chaotic dynamics. *Journal of Physics: Conference Series* 692(1), 2016 [https://doi.org/10.1088/1742-6596/692/1/012011].
- [8] Haliuk S. et. al.: Circuit implementation of Lozi ring-coupled map. *Proc. of 4th International Scientific-Practical Conference Problems of Infocommunications. Science and Technology*, Kharkiv, 2017, 249–252 [https://doi.org/10.1109/INFOCOMMST.2017.8246390].
- [9] Kocarev L. et. al.: *Chaos-Based Cryptography Theory, Algorithms and Applications*. Springer 2011 [https://doi.org/10.1007/978-3-642-20542-2].
- [10] Krulikovskiy O. et. al.: PRNG based on modified Tratas chaotic system. *Modern information security* 2, 2016, 69–77 [http://nbuv.gov.ua/UJRN/szi\_2016\_2\_12].
- [11] Krulikovskiy O. et. al.: Testing timeseries ring-coupled map generated by on FPGA. *Telecommunication and Informative Technologies* 4, 2016, 24–29.
- [12] Krulikovskiy O., Haliuk S.: Periodicity of Timeseries Generated by Logistic Map. Part I. *Security of Infocommunication Systems and Internet of Things* 1(2), 2023, 02010 [https://doi.org/10.31861/sisiot2023.2.02010].
- [13] Lozi R.: Survey of Recent Applications of the Chaotic Lozi Map. *Algorithms* 16(491), 2023 [https://doi.org/10.3390/a16100491].
- [14] Machicao J., Bruno O. M.: Improving the pseudo-randomness properties of chaotic maps using deep-zoom. *Chaos* 27(5), 2017, 053116 [https://doi.org/10.1063/1.4983836].
- [15] National Institute of Standards and Technology. *A Statistical Test Suite for Random and Pseudorandom Number Generators for Cryptographic Applications*, NIST Spec. Publication 800-22, Rev. 1a, 2010.

- [16] Rodriguez-Vazquez A. et. al.: Chaos from Switched-Capacitor Circuits: Discrete Maps, Proc. of the IEEE, Special Issue on Chaotic Systems 75(8), 1987, 1090–1106 [https://doi.org/10.1109/PROC.1987.13852].
- [17] Shujun L. et. al.: On the dynamical degradation of digital piecewise linear chaotic maps. International Journal of Bifurcation and Chaos 5(10), 2005, 3119–3151 [https://doi.org/10.1142/S0218127405014052].
- [18] The Marsaglia Random Number CDROM including the Diehard Battery of Tests of Randomness (accessed: 19.03.2024) [https://web.archive.org/web/20160125103112/http://stat.fsu.edu/pub/diehard/].
- [19] Vázquez-Medina R. et. al.: Design of chaotic analog noise generators with logistic map and MOS QT circuits. Chaos, Solitons & Fractals 40(4), 2009, 1779–1793 [https://doi.org/10.1016/j.chaos.2007.09.088].
- [20] Wang X. et. al.: A New Four-Dimensional Chaotic System and its Circuit Implementation. Frontiers in Physics 10, 2022 [https://doi.org/10.3389/fphy.2022.906138].
- [21] Wang Z., Liu S.: Design and Implementation of Simplified Symmetry Chaotic Circuit. Symmetry 14, 2022, 2299 [https://doi.org/10.3390/sym14112299].
- [22] Wong D.: Real-World Cryptography. Manning, 2021.
- [23] Yuan G., Yorke J. A.: Collapsing of chaos in one dimensional maps. Physica D – 136, 2000, 18–30 [https://doi.org/10.1016/S0167-2789(99)00147-5].

**Ph.D. Oleh Krulikovskyi**

e-mail: o.krulikovskyi@chnu.edu.ua

Assistant professor at Radio Engineering and Information Security Department of Chernivtsi National University. His research field covers digital signal processing, FPGA and hardware cryptography. Author of more than 20 publications.



<https://orcid.org/0000-0003-3836-2675>

**Ph.D. Serhii Haliuk**

e-mail: s.haliuk@chnu.edu.ua

Assistant professor at Radio Engineering and Information Security Department of Chernivtsi National University. His research interest covers chaotic communication, cryptography, signal processing, circuit design. Author of more than 40 publications.

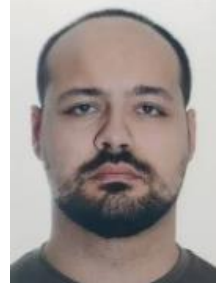


<https://orcid.org/0000-0001-5995-6857>

**M.Sc. Ihor Safronov**

e-mail: safronov.ihor@chnu.edu.ua

Ph.D. student at Radio Engineering and Information Security Department of Yuriy Fedkovych Chernivtsi National University. His research field covers digital signal processing, PCB layout and circuit design.



<https://orcid.org/0009-0009-9349-8349>

**Ph.D. Valentyn Lesynskyi**

e-mail: lesynskyi@chnu.edu.ua

Associate professor, Radio Engineering and Information Security Department of Yuriy Fedkovych Chernivtsi National University. His research interest includes energy-efficient technologies, circuit design, power electronics, motion control and mechatronics.



<https://orcid.org/0000-0002-1259-1974>